Barium Titanate Based Acoustic Sensing Elements

Nefeli Motsi[1*], Nikolaos Siafakas[1], Athanasios Mamalis[2], Evangelos Hristoforou[1]

[1]*School of Electrical and Computer Engineering, National Technical University of Athens, Greece*
[2]*Project Center for Nanotechnology and Advanced Engineering (PC-NAE), Greece*
[*]*Email: nefelimotsi@mail.ntua.gr*

Piezoelectric materials like PZT and $BaTiO_3$ find application in various fields, in-cluding supercapacitors, dielectrics, ceramics, and catalysts [1, 2]. Barium ti-tanate ($BaTiO_3$) offers numerous advantages in terms of its structural, piezoelec-tric and ferroelectric properties [3]. Nevertheless, to enhance these characteristics, barium was substituted with strontium using both sintering and sol-gel methods. Barium strontium titanate (BST) ferroelectric material have attracted considerable attention due to its chemical stability, high permittivity, excellent tunability, and minimal dielectric losses [4]. In this research, we study the synthesis of perov-skite $Ba_xSr_{(1-x)}TiO_3$, with varying strontium content from 0% to 50%, using sin-tering and sol-gel method. Additionally, all samples underwent further examina-tion through several techniques, such as Scanning Electron Microscope (SEM), X-ray Diffraction (XRD), Differential Thermal Analysis (DTA) and Thermo-gravimetric Analysis (TGA).

Keywords: BST, piezoelectric materials, $Ba_xSr_{(1-x)}TiO_3$, sintering, sol-gel.

1. Introduction

Barium titanate ($BaTiO_3$), a commonly used type of electronic ceramic material, possesses a high dielectric constant and low dielectric loss, rendering it a superb mate-rial for electronic applications [5-9]. These attributes make it an excellent option for a variety of electronic uses, including multilayer ceramic capacitors (MLCCs), positive temperature coefficient of resistivity (PTCR) thermistors, dynamic random-access memories (DRAM), and piezoelectric sensors, thanks to its outstanding features such as a high permittivity and impressive ferroelectric and piezoelectric properties [10-12].

The development of ceramic powders' microstructure and performance is significantly affected by the method utilized. The choice of manufacturing technique has a substantial influence on the characteristics and properties displayed by the eventual ceramic products. Within the field of electroceramics, there is a growing interest in discovering novel methods to enhance the properties of $BaTiO_3$ powders. The traditional approach for producing $BaTiO_3$ involves a solid-state reaction carried out at elevated temperatures exceeding 900°C, using TiO_2 and $BaCO_3$ as raw materials. However, this often results in powders that tend to aggregate, disperse unevenly, and possess low purity, leading to uncontrolled morphologies and poor electrical proper-ties in the final sintered product [13, 14]. In recent times, attention has shifted towards the sol-gel technique for fabricating $BaTiO_3$ powders due to its ability to provide mild reaction conditions and produce powders with high purity, excellent particle distribution, precise composition control, and homogeneity.

While $BaTiO_3$ possesses numerous advantages in terms of its structural and pie-zoelectrical characteristics, efforts have been made to improve the sensitivity and response of the final product by substituting barium with strontium using both sintering and sol-gel methods, leading to the development of barium strontium titanate (BST) material. The ferroelectric and dielectric properties of BST ceramics are subject to significant influence from various factors including sintering conditions, grain size, porosity, doping levels, and structural defects. This suggests that optimizing the doping and sintering conditions holds promise as an approach to enhance the dielectric properties of BST ceramics [15].

Barium strontium titanate ($Ba_xSr_{1-x}Ti0_3$) is a solid solution that combines the properties of barium titanate ($BaTi0_3$) and strontium titanate ($SrTi0_3$). $BaTiO_3$ demonstrates ferroelectric behavior with a Curie temperature (Tc) of 120°C, while $SrTiO_3$ lacks ferroelectric properties and does not undergo a ferroelectric phase transition [16]. The Curie temperature of $BaTiO_3$ decreases linearly as Ba^{2+} ions are substituted with Sr^{2+} ions, decreasing at a rate of 3.7°C per mole percentage of substitution. In bulk BST, the Curie temperature can range from -232°C to 127°C, depending on the specific ratio of barium to strontium within the material [17].

The conventional solid-state reaction method is less than ideal for producing high-performance Barium Strontium Titanate (BST) powders because it necessitates high calcination temperatures (900-1100°C). Consequently, it is imperative to investigate alternative synthesis methods, such as the sol-gel technique, to attain the desired qualities in BST powders. Recent research has focused extensively on the sol-gel process due to its remarkable effectiveness in generating ceramic powders that exhibit high purity, small particle sizes, uniformity, and the ability to be sintered at lower temperatures [18, 19].

To identify the method that produces the most favorable end products, this study included the synthesis of $Ba_xSr_{(1-x)}TiO_3$ with different Sr content levels, spanning from 0% to 50%, using both techniques. Subsequently, various characterization methods were applied to assess and contrast the structure and properties of the resulting mate-rials.

2. Materials and methods

The synthesis of $Ba_xSr_{(1-x)}TiO_3$ materials via the sintering process initiated with a powder blend consisting of barium carbonate ($BaCO_3$), strontium carbonate ($SrCO_3$), and titanium dioxide (TiO_2). This powder mixture underwent a ball milling procedure in distilled water. Later on, all the samples were subjected to Differential Thermal Analysis (DTA) to identify the temperatures at which the reactions resulting in the formation of $BaCO_3$ and $SrCO_3$ took place. These analyses were carried out within the temperature range of 50-1300°C, with a heating rate of 2°C per minute. Following this, the calcined powders were subjected to isostatic pressing at a pressure of 200 MPa using a cold isostatic press, resulting in the formation of discs weighing 3 grams, with a diameter of 3 cm and a width of 1.5 mm. The cold isostatic process guarantees a uniform and enhanced compaction of the final products. Subsequently, these discs were sintered at 1500°C for a duration of 4 hours in an air atmosphere.

The raw materials employed for synthesizing $Ba_xSr_{(1-x)}TiO_3$ through the sol-gel method consisted of barium acetate ($Ba(CH_3COO)_2$), strontium acetate ($Sr(CH_3COO)_2$), and titanium isopropoxide ($Ti(OC_3H_7)_4$). Solvents such as acetic acid (CH_3COOH), acetylacetone ($CH_3COCH_2COCH_3$), and propylene glycol ($C_3H_8O_2$) were used, with distilled water serving as an additional agent. All chemicals used in the experiment were of analytical grade and were employed without further treatment. The process began with the preparation of solutions, which were then calcinated at 120°C to produce xerogels. Subsequently, these xerogels underwent Thermo-gravimetric Analysis (TGA) and Differential Thermal Analysis (DTA) to measure the weight changes of the samples across a temperature range and identify the temperatures at which reactions leading to the formation of $BaTiO_3$ and $SrCO_3$ occurred. These analyses were conducted in the temperature range of 50-1300°C at a heating rate of 2°C/min. The calcined xerogels were further processed by sintering at 750°C for 90 minutes at a heating rate of 5°C/min in an air atmosphere. Following this, the calcined xerogels were subjected to isostatic pressing at a pressure of 200 MPa using a cold isostatic press to create discs weighing 3 grams, with a diameter of 3 cm and a width of 1.5 mm. Finally, these discs were sintered at 1500°C for 2 hours.

All the samples produced using both the sintering and sol-gel methods were subjected to examination through X-ray diffraction (XRD) and scanning electron microscopy (SEM).

3. Results

3.1Thermogravimetry Differential Thermal Analysis (TG/DTA)

In Figures 1 and 2, on the DTA graphs, the points where the sample undergoes a phase change or reacts are characterized by the release or absorption of thermal energy. This results in a difference in temperature between the sample and the reference sample, even though both receive the same amount of thermal energy. This temperature difference persists as long as the phase change or reaction continues, and then the sample returns to thermal equilibrium with the reference sample. These discrepancies are measured and presented in a diagram, enabling the determination of the temperature at which this phenomenon occurs and the temperature range over which it extends. This information is incredibly valuable as it provides precise insights into the necessary calcination temperature for achieving the desired final products. In both cases, $BaCO_3$ was mixed with TiO_2, and $SrCO_3$ was blended with

TiO_2 in a 1:1 mole ratio, allowing for meticulous control over the composition during the calcination process.

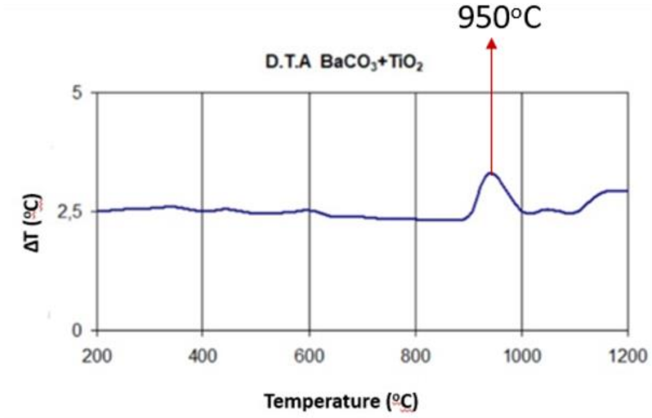

Fig. 1. DTA of $BaCO_3$ powder made by sintering.

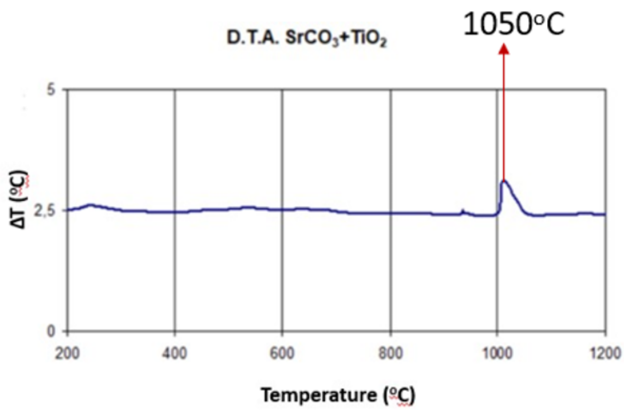

Fig. 2. DTA of $SrCO_3$ powder made by sintering.

Following the thermal analysis, which included TG, DTG, and DTA conducted on xerogels with 0% and 50% Sr content, several diagrams (Figures 3 and 4) were generated to identify the temperatures at which the breakdown of organic materials occurs and the reactions leading to the formation of BST. These analyses were carried out within the temperature range of 50-1300°C at a heating rate of 2°C/min. Up to ap-proximately 160°C, the analysis showed the vaporization of water and other liquids. Below 300°C, the vaporization of deposits from organic solutions onto the xerogel powder occurred. The peaks observed in the DTA curve correspond to the decomposition of carboxyls and alkoxides. In the temperature range between 300 and 400°C, carbides and oxides such as $BaCO_3$ and TiO_2 were formed. Subsequently, a solid-phase reaction occurred:

$$(Ba_xSr_{(1-x)})CO_3+TiO_2 \rightarrow (Ba_xSr_{(1-x)})TiO_3+CO_2$$

The transition to the desired perovskite form of BST is achieved when temperatures reach between 450°C and 550°C. During this range, the plateau observed in the analysis indicates a loss of mass, corresponding to the peaks seen in the DTA curve. The experimental mass loss recorded in the BaTiO3 (0% Sr) plot between 550°C and 720°C amounts to 13.4%. In the case of $Ba_xSr_{(1-x)}TiO_3$ with 50% Sr, the experimental mass loss during the same temperature range is 16.1%. These values are close to the theoretical mass losses for the desired crystal compositions, which are 15.5% and 17.2%, respectively.

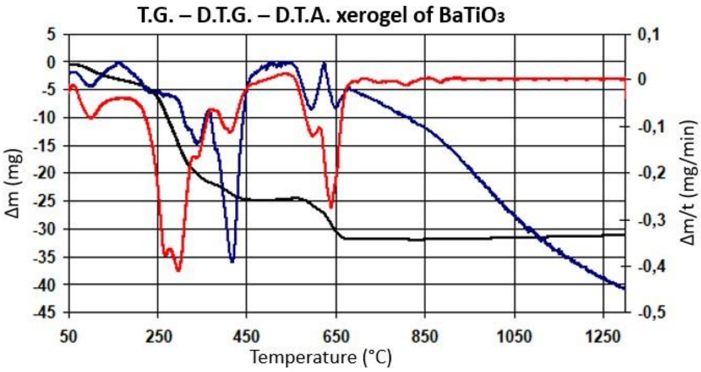

Fig. 3. Graphs of T.G. (black line), D.T.G (red line). and D.T.A. (blue line) of xerogel of Ba-TiO_3.

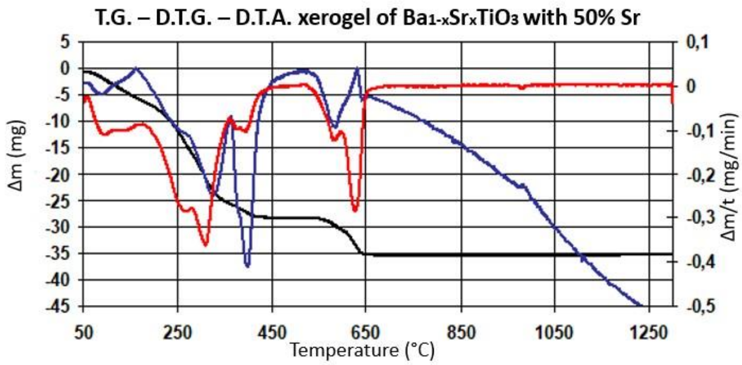

Fig. 4. Graphs of T.G. (black line), D.T.G (red line). and D.T.A. (blue line) of xerogel of $Ba_{(1-x)}Sr_xTiO_3$ with 50% Sr.

3.2Structure and morphology

Based on the XRD graphs presented in Figures 5 and 6, it is evident that all samples produced through both the sintering and sol-gel methods exhibit a perovskite structure, with a predominant crystalline orientation towards the [111] crystallographic axis across all the various concentrations of Sr. These observations strongly indicate the successful formation of barium-strontium titanate (BST) in the samples. In some specific samples of $Ba_xSr_{(1-x)}TiO_3$ consisted of 30% Sr and 50% Sr, produced through the sintering process (as depicted in Figure 5b and 5c, respectively), the presence of a peak corresponding to $SrTiO_3$ suggests an unsuccessful mixing of the $BaCO_3$ and $SrCO_3$ powders prior to calcination. This indicates that the desired chemical reaction to form the BST compound was not achieved in these particular samples, resulting in the presence of $SrTiO_3$.

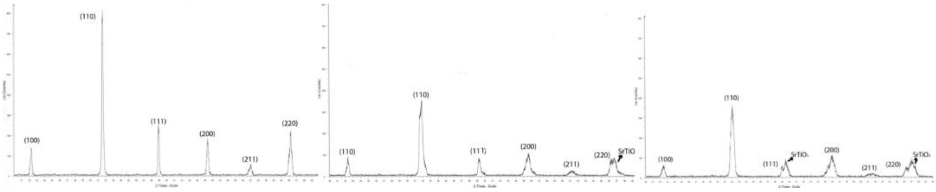

(a) (b) (c)

Fig. 5. XRD diagrams of $Ba_xSr_{(1-x)}TiO_3$ for (a) 0% Sr; (b) 30% Sr and c) 50% Sr developed by sintering.

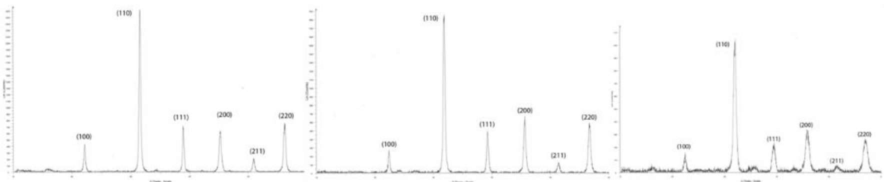

(a) (b) (c)

Fig. 6. XRD diagrams of $Ba_xSr_{(1-x)}TiO_3$ for (a) 0% Sr; (b) 30% Sr and (c) 50% Sr developed by sol-gel.

Figures 7 and 8 display SEM micrographs of $Ba_xSr_{(1-x)}TiO_3$ samples containing 0%, 30%, and 50% Sr, which were developed using both the sintering and sol-gel methods, respectively. In the case of the sintering process, it is evident that the materials exhibit uniform microstructures with the formation of necks between particles. On the other hand, samples prepared through the sol-gel method show nonuniform microstructures with the presence of aggregations. As the Sr content increases in the BST material, the microstructure appears to improve and become more uniform. This suggests that higher Sr concentrations may have a beneficial effect on the microstructural properties of the material, potentially leading to enhanced performance in certain applications.

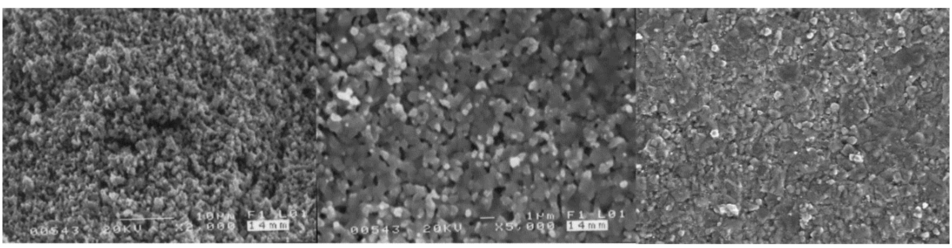

(a) (b) (c)

Fig. 7. SEM micrographs of $Ba_xSr_{(1-x)}TiO_3$ with (a) 0% Sr; (b) 30% Sr and (c) 50% Sr developed by sintering.

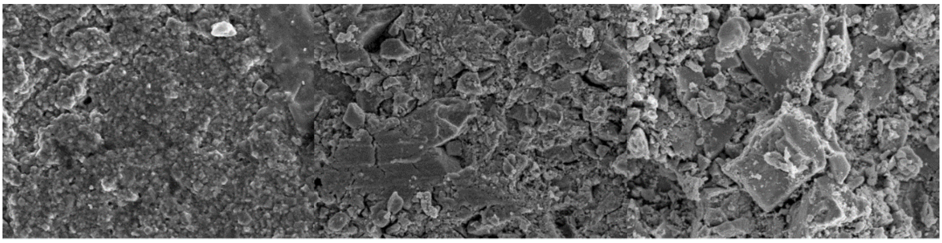

(a) (b) (c)

Fig. 8. SEM micrographs of $Ba_xSr_{(1-x)}TiO_3$ with (a) 0% Sr; (b) 30% Sr and (c) 50% Sr developed by sol-gel.

4. Discussion

Based on the Differential Thermal Analysis (DTA) and Thermogravimetric Analysis (TGA) illustrated in Figures 1 and 2, which were carried out within the temperature range of 50-1300°C at a heating rate of 2°C/min, it is observed that the reaction leading to the formation of $BaTiO_3$ occurs at 950°C, and the reaction leading to the formation of $SrTiO_3$ takes place at 1050°C for the samples produced via the sintering method. Figures 3 and 4 provide additional insights into the thermal analysis. Above approximately 160°C, there is evidence of water and other liquids vaporizing. Below 300°C, the vaporization of deposits from organic solutions onto the xerogel powder occurs. The peaks observed in the DTA curve correspond to the decomposition of carboxyls and alkoxides. In the temperature range between 300°C and 400°C, carbides and oxides, such as $BaCO_3$ and TiO_2, are formed. Subsequently, the desired perovskite form of BST was successfully produced via the sol-gel method.

Between 450°C and 550°C, the plateau observed indicates a mass loss that accompanies the corresponding peaks in the DTA curve. The experimental mass loss in the plot for $BaTiO_3$ (0% Sr) and in $Ba_xSr_{(1-x)}TiO_3$ with 50% Sr between 550°C and 720°C is measured at 13.4% and 16.1%, respectively. The XRD graphs presented in Figures 5 and 6 reveal that all samples, regardless of whether they were developed through the sintering or sol-gel method, exhibit a perovskite structure. Furthermore, there is a predominating crystalline orientation towards the [111] crystallographic axis across all the different concentrations of Sr. This indicates the successful formation of barium-strontium titanate (BST) in all these samples. However, in the case of $Ba_xSr_{(1-x)}TiO_3$ with 30% and 50% Sr produced through the sintering process, the presence of peaks corresponding to $SrTiO_3$ suggests either a high supply of Sr or an ineffective mixing of the $BaCO_3$ and $SrCO_3$ powders prior to calcination. Notably, increasing the Sr concentration in the material appears to promote more effective microcrystallization. The wider peaks observed might have resulted from the higher utilization of Sr, which induces intense heterogeneous nucleation, leading to an in-creased number of crystals produced. Figures 7 and 8 demonstrate SEM micrographs of $Ba_xSr_{(1-x)}TiO_3$ samples developed through both the sintering and sol-gel methods, respectively. In the case of the sintering process, it is evident that the materials exhibit uniform microstructures with the formation of necks between particles. This indicates a high level of cohesion and homogeneity in the material. On the other hand, samples prepared via the sol-gel method show a nonuniform microstructure with the presence of aggregations or uneven distribution of particles. This suggests that the sol-gel method may result in a less uniform microstructure compared to sintering. Interestingly, as the concentration of Sr increases in the BST material, the microstructure appears to improve and become more uniform. This indicates that higher Sr concentrations may have a positive impact on the microstructural properties of the material, potentially leading to enhanced performance in certain applications. The next step in the process involves the creation of metal contacts through techniques like sputtering or PVD (Physical Vapor Deposition). This process is necessary in order to assess the electrical characteristics of the prepared material. The plan is to measure the overall impedance of the material and examine how it varies with temperature and the dielectric constant. Additionally, the goal is to determine the Curie temperature, which is the temperature at which the ferroelectric material transitions to a paraelectric phase. These measurements and analyses are crucial for understanding the electrical behavior and properties of the material in various conditions.

5. Conclusions

In this study, $Ba_xSr_{(1-x)}TiO_3$ materials with Sr concentrations ranging from 0% to 50% were produced using both the sintering and sol-gel methods. These materials underwent characterization techniques including TGA, DTA, XRD, and SEM. For the materials produced through the sintering method, DTA revealed that the reaction leading to the formation of $BaTiO_3$ occurs at 950°C (as shown in Figure 1), while the reaction leading to the formation of $SrTiO_3$ takes place at 1050°C (as depicted in Figure 2). Regarding BST materials developed via the sol-gel method, TGA analysis demonstrated that between the temperature range of 550°C and 720°C, the experimental mass loss for $BaTiO_3$ was measured at 13.4%, whereas for $Ba_xSr_{(1-x)}TiO_3$ with 50% Sr, it was found to be 16.1%. These findings provide valuable insights into the thermal behavior and composition of the materials.

The BST materials developed through the sintering method exhibit a more uniform microstructure with the formation of necks between particles. On the other hand, the samples developed through the sol-gel method display a nonuniform microstructure with the presence of aggregations or uneven distribution of particles. However, an interesting trend emerges as the concentration of Sr increases in the BST material, where the microstructure appears to improve and become more uniform. This suggests that higher Sr concentrations may contribute to enhanced microstructural properties, leading to a more homogeneous material. Considering the XRD characterization and the microstructural observations, it appears that the sol-gel method produces samples with superior crystallography and, to some extent, improved microstructure compared to those developed by sintering. These findings suggest that the sol-gel method is preferable in this context. The advantages of the sol-gel method include the production of ceramic powders that are purer, smaller in size, and more uniform. Additionally, the sol-gel method allows for sintering at lower temperatures compared to traditional sintering processes. These benefits make the sol-gel method an effective choice for achieving high-quality ceramic materials with desirable properties.

Acknowledgement

This research has been co-financed by European Union and Greek national funds through the Regional Operational Program Sterea Ellada 2014-2020 under the call “Support of Plans for Research, Technological Development, and Innovation in RIS3 sectors of the Region of Sterea Ellada (project code: ΣTEP1-0025535).

References

1. Ullah, A., et al., *Large electromechanical response in lead-free La-doped BNKT–BST piezoelectric ceramics.* Journal of the American Ceramic Society, 2014. **97**(8): p. 2471-2478.
2. Dineva, P., et al., *Piezoelectric materials*. 2014: Springer.
3. Jain, A., Y. Wang, and L. Shi, *Recent developments in BaTiO3 based lead-free materials for energy storage applications.* Journal of Alloys and Compounds, 2022. **928**: p. 167066.
4. Enhessari, M., et al., *Synthesis and characterization of barium strontium Titanate (BST) micro/nanostructures prepared by improved methods.* 2011.
5. Duong, N.X., et al., *Polymorphic phase transition in BaTiO3 by Ni doping.* Ceramics International, 2019. **45**(13): p. 16305-16310.
6. Verma, K. and S. Sharma, *Influence of addition of copper cadmium ferrite on the dielectric and electrical behavior of BaSrTiO3 ceramics.* Ceramics International, 2012. **38**(7): p. 5957-5966.
7. Slimani, Y., et al., *Frequency and dc bias voltage dependent dielectric properties and electrical conductivity of BaTiO3SrTiO3/(SiO2) x nanocomposites.* Ceramics International, 2019. **45**(9): p. 11989-12000.
8. Mi, L., et al., *Synthesis of BaTiO3 nanoparticles by sol-gel assisted solid phase method and its formation mechanism and photocatalytic activity.* Ceramics International, 2020. **46**(8): p. 10619-10633.
9. Fuentes, S., et al., *Influence of reactant type on the Sr incorporation grade and structural characteristics of Ba1− xSrxTiO3 (x= 0− 1) grown by sol–gel-hydrothermal synthesis.* Ceramics International, 2013. **39**(8): p. 8823-8831.
10. Chen, C., et al., *Hydrothermal synthesis of BaTiO3: Crystal phase and the Ba2+ ions leaching behavior in aqueous medium.* Materials Chemistry and Physics, 2008. **110**(1): p. 186-191.
11. Wang, W., et al., *Low-temperature synthesis of BaTiO3 powders by the sol–gel-hydrothermal method.* Ceramics International, 2013. **39**(6): p. 7127-7134.
12. Wang, Y., et al., *Hydrothermal synthesis of single-crystal BaTiO3 dendrites.* Materials Letters, 2009. **63**(2): p. 239-241.
13. Zhang, Y., L. Wang, and D. Xue, *Molten salt route of well dispersive barium titanate nanoparticles.* Powder technology, 2012. **217**: p. 629-633.
14. Zhu, X., et al., *Hydrothermal synthesis of nanocrystalline BaTiO3 particles and structural characterization by high-resolution transmission electron microscopy.* Journal of crystal growth, 2008. **310**(2): p. 434-441.
15. Reddy, S.B., K.P. Rao, and M.R. Rao, *Effect of La substitution on the structural and*

dielectric properties of BaZr0. 1Ti0. 9O3 ceramics. Journal of alloys and compounds, 2009. **481**(1-2): p. 692-696.
16. Gatea, H.A., *Synthesis and characterization of BaSrTiO3 perovskite thin films prepared by sol gel technique.* International Journal of Thin Film Science and Technology, 2021. **10**(2): p. 5.
17. Kathait, G.S., et al., *Effect of different strontium content on dielectric properties of barium strontium titanate ceramic.* Int. J. Latest Technol. Eng. Manage. Appl. Sci, 2017. **6**: p. 75.
18. Cernea, M., et al., *Sol–gel synthesis and characterization of BaTiO3-doped (Bi0. 5Na0. 5) TiO3 piezoelectric ceramics.* Journal of Alloys and Compounds, 2010. **490**(1-2): p. 690-694.
19. Li, W., et al., *Sol–gel synthesis and characterization of Ba (1− x) SrxTiO3 ceramics.* Journal of Alloys and Compounds, 2010. **499**(2): p. 255-258.